International Journal of Heat and Mass Transfer 240 (2025) 126638

Contents lists available at ScienceDirect

International Journal of Heat and Mass Transfer

journal homepage: www.elsevier.com/locate/ijhmt

Interplay of flow stratification, segregation channels, and crystal dynamics in a solidifying aqueous ammonium chloride solution

Andreas Ludwig [a,*], Golshan Shayesteh [a], Mihaela Stefan-Kharicha [a], Menghuai Wu [a], Abdellah Kharicha [a,b]

[a] Metallurgy Department, Montanuniversitaet Leoben, Leoben, Austria
[b] CD Laboratory for Magnetohydrodynamic Application in Metallurgy, Montanuniversitaet Leoben, Leoben, Austria

ARTICLE INFO

Keywords:
Solidification
Segregation
Flow channels
Solutal buoyancy
Double-diffusive convection
Crystal multiplication
Sedimentation

ABSTRACT

An experimental investigation of the solidification dynamics of an aqueous ammonium chloride solution conducted using a relatively large rectangular test cell subject to vertical side cooling reveals several interesting phenomena. Besides the well-known concentration and flow stratification at the top part of the test cell, an increasing number of equiaxed crystals affects both the growth of the vertical mushy layer as well as the flow in the bulk melt. The rising melt flow in the solidifying mushy zone creates segregation channels and leads to the formation of indentations (bowl-shaped depressions) in the mushy zone layer at the exits of these channels. Crystals that descend along the forefront of the mushy layer may either stick to protruding dendrite tips or sediment onto the lower edges of the indentations. These processes lead to crystal agglomerations that collapse when getting too large. The subsequent impact of the sliding-down crystals with lower mushy zone regions leads to further fragmentation. The corresponding crystal sedimentation is thus irregular and layers of sediment occur rather than a uniform sedimentation bed. These observations are relevant in fields such as metallurgy, materials and environmental science, and geology, and could enhance the design of industrial processes and contribute to natural system modeling.

1. Introduction

Observations of solidification processes using transparent model systems have been quite useful in understanding the formation of the microstructure of an alloy. Studies on the solid/liquid (s/l) interface morphology and its dynamic were done using organic materials that reveal one or two high-temperature non-facetted phases. For example, groundbreaking experimental results on dendritic growth were obtained by Huang and Glicksman using succinonitrile (SCN) [1]. Jackson and Hunt studied coupled eutectic growth using tetrabromethane-hexachloroethane (CBr_4—C_2Cl_6) [2,3]. A review that demonstrates the importance of using transparent organic materials to understand the solidification dynamics of metallic alloy melts can be found in [4].

Flow-related phenomena that occur during solidification have been studied using aqueous ammonium chloride solutions (NH_4Cl-H_2O) with <80.3 wt.% H_2O. Due to the low entropy of fusion of ammonium chloride, this material solidifies very much like metallic alloys. It forms a columnar dendritic network and equiaxed dendrites with a sixfold symmetry. With the help of direct observations using NH_4Cl-H_2O solutions, Copley et al. found in 1970 that freckles in solidified castings are caused by upward-flowing liquid jets [5]. In the same year, McDonald and Hunt suggested a mechanism that explains the formation of A-segregation, again based on observations of NH_4Cl-H_2O solutions [6]. In 1978, Szekely and Jassal observed solidification with convection (natural and forced) in a rectangular container that was cooled from one side [7]. More experiments with different geometries were done around 1982 by Ohno et al. [8–10]. Similar work as the one performed by Copley et al. [5] was done by Sample and Hellawell in 1982/1984 [11,12]. They elaborated on the ideas behind freckle formation.

In 1988/89, two groups studied the solidification/melting of NH_4Cl-H_2O solutions in rectangular cavities: Beckermann and Viskanta [13–15] and Christenson and Incropera et al. [16,17]. They showed that solutally driven flow strongly influences solidification rates, localized remelting, and macroscopic solute redistribution. For aqueous ammonium chloride solutions with a composition of <80.3 wt.% H_2O,

* Corresponding author.
E-mail address: ludwig@unileoben.ac.at (A. Ludwig).

https://doi.org/10.1016/j.ijheatmasstransfer.2024.126638
Received 24 October 2024; Received in revised form 9 December 2024; Accepted 23 December 2024
Available online 27 December 2024

solidification starts with the formation of NH_4Cl crystals that reject H_2O. Therefore, the segregated interdendritic liquid is enriched in H_2O and thus lighter than the initial melt. Solutal buoyancy flow is the consequence. The aforementioned studies showed that with side-cooling of such a solution, solidification happens along the cooled sidewall while a variety of double-diffusive convection phenomena in the liquid occur, including plumes, and flow and concentration stratifications. Even remelting in parts of the system could be observed.

Because of the unstable density layering in solidifying NH_4Cl-H_2O mixtures, such solutions were frequently used to study channel formation in partly solidified systems. Chen and Chen in 1991 [18], Hellawell et al. [19], and Magril and Incropera [20] in 1993 could further elucidate how and why plumes and freckles form. Especially, in ref. [19] it is discussed that boundary layer perturbations lead to the onset of plumes and in ref. [20] it is shown that in this unidirectional solidification configuration plumes also lead to double-diffusive layers in the upper part of the test cell. In Worster's 1997 review, existing knowledge on convection in mushy layers was compiled [21].

Gao and Wang [22] investigated the effect of crystal sedimentation on the columnar-to-equiaxed transition by using NH_4Cl-H_2O solutions and applying cooling from the top, similar to Ohno's work [10]. This resulted in unidirectional columnar crystals growing downward. Ahead of the columnar front, equiaxed crystals were observed that had most probably originated by fragmentation of the columnar dendrites in the presence of thermal convection. Sinking of these equiaxed crystals finally led to the formation of a sedimented layer of crystals. A similar topic was addressed by Zhong et al. [23] but using a much larger cylindrical test cell. They called the massive crystal sedimentation from the cooled top 'crystal rain' similar to the 'showering from the surface' as reported in ref. [24]. Recently, Thakur et al. [25,26] measured simultaneously temperature and salt concentration distributions during unidirectional solidification of NH_4Cl-H_2O solutions where also double-diffusive layering occurs.

The group of the present authors reported in 2017 [27] about the massive formation of equiaxed crystals by sliding down mushy zone segments. They called this phenomenon 'crystal avalanche' as it resembles similar phenomena known from mountain regions. The important difference to all other studies on the solidification of NH_4Cl-H_2O solutions was the utilization of a relatively large test cell of inside dimensions of 60 cm in height (h), 40 cm in width (w), and 6 cm in depth (d) cooled from the two narrow sidewalls. Note that e.g. Beckermann's vertical rectangular test cell had inside dimensions of only 4.76 cm in height and width and 3.81 cm in depth [15]. The test cell used by Christenson and Incropera et al. had a height of 14.4 cm [16,17]. The present work is continuing the experimental studies on crystal avalanches applying again the relatively large test cells used in ref. [27]. As will be discussed later, the size of the test cell is crucial for the occurrence of phenomena that lead to the sliding down of multiple crystals. Even when applying medium-sized test cells, like the one used to study the melt flow and motion of equiaxed crystals during solidification using a dual phase PIV technique (h/w/d 10 × 10 × 1 cm^3) [28,29], sliding downward phenomena were not reported.

The experimental procedure applied in this work has also been described in a previous conference proceeding [30], where the four stages of the present solidification process have been defined and the mechanism of loosening and sliding down of mushy zone segments was addressed. In the present contribution, we are showing that the concentration and flow stratification that is caused by interdendritic flow channels interact with the increasing amount of equiaxed crystals. Not only the loosening and sliding down of mushy zone segments is responsible for avalanche-type phenomena but also the collapsing of crystal agglomerations that form at different locations along the vertical mushy layer. So to understand the occurrence of the uneven sedimentation layering at the bottom of the test cell, the interplay of flow stratification, segregation channels, and crystal dynamics must be considered.

2. Experimental procedure

The solidification experiment described in this work was performed using the test cell shown in Fig. 1. Cooling was performed only on the two metallic narrow sidewalls. A solution containing NH_4Cl −70.5 wt.% H_2O was applied. The entire solidification process was recorded using a centrally positioned optical camera (Canon EOS R6) that captured pictures with a size of 5472 × 3648 px every second. The relevant part of the pictures showing the test cell had a size of 2211 × 2821 px. From the corresponding video that is available as supplementary material, the occurrence and motion of crystals, the solidification dynamics of the vertical mushy layer, and the formation of sedimentation layers at the bottom region were detected. The inside dimensions of the test cell were 60 cm in height, 40 cm in width, and 6 cm in depth. The lateral and bottom walls were constructed using brass, and the front and back walls were made of commercial polymethylmethacrylate (PMMA) plates. The PMMA windows were sealed against the brass walls using a rubber gasket. Therefore, a small gap existed between the plexiglass and the brass wall. Within the brass sidewalls, cooling channels were designed with a meander pattern to ensure a uniform temperature distribution of the brass. The temperature was maintained by circulating water at a predetermined temperature through these channels. So, the cooling was governed by the bath thermostat that was used to adjust the circulating water temperature.

For the experiment presented here, the NH_4Cl-H_2O solution was produced directly inside the test cell with NH_4Cl that had a purity of +99.7 pct. A corresponding amount of NH_4Cl powder was stirred into distilled water and heated for approximately 1 hour until the powder was fully dissolved. After that, air bubbles that adhered to the plexiglass walls were removed using a wiper. However, it was difficult to completely remove all air bubbles. Then the test cell was covered with a glass plate and left untouched for 1 h so that the mechanically introduced convection could fade away. A filling height of 55 cm was chosen. Based on the NH_4Cl-H_2O phase diagram [31], the liquidus temperature of a solution with 70.5 wt.% H_2O is $T_l = 31.5$ °C (304.6 K). The initial temperature of the brass sidewalls was set to $T_0 = 60$ °C (333 K). During the process, the sidewalls were cooled down to $T_{inf} = 5$ °C (278 K) with a nearly constant cooling rate of 0.8 K/min. Six thermocouples were placed within the brass walls at different positions (A, B, C, D, E, and F); one thermocouple measured the temperature inside the solution (G); and the last measured the temperature at the plexiglass surface outside the test cell (H). It should be mentioned that an NH_4Cl-H_2O solution with 70.5 wt.% H_2O would completely solidify at the eutectic temperature of $T_E = -15.4$ °C (257.2 K) [31]. With the lowest temperature of 5 °C at the narrow sidewalls and with a temperature of approximately 27 °C inside the solution at position G (see Fig. 1), it is clear that the solution in the test cell did not solidify completely. Further cooling to 0 °C or even below would lead to air moisture condensation at the plexiglass windows. To avoid that, 5 °C was chosen as the minimal temperature for cooling.

An experiment like the one presented here lasted around 4 h. With the framerate of 1 fps around 140.000 pictures were recorded which resulted in 111 GB data. Subsequently, the relevant part of the pictures was cropped. To increase contrast and sharpness, the pictures were further processed by using MATLAB.[c] Unfortunately, this procedure also highlights the remaining air bubbles adhering to the plexiglass sidewalls leaving behind a falsified impression of a significant amount of bubbles.

We also varied the composition of the solution, bath height, and cooling intensity and used a double-color PIV system to get quantitative measurements of the strength of the flow dynamics. The corresponding results would overload the present report and will thus be presented in an upcoming publication.

[c] https://www.mathworks.com/products/matlab.html

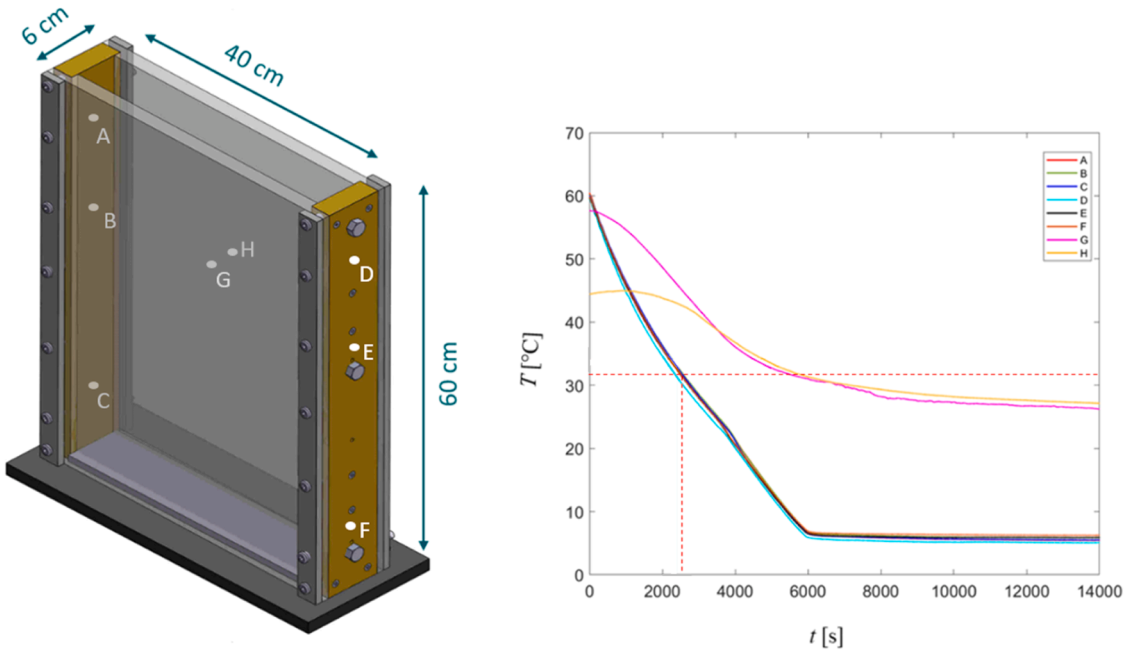

Fig. 1. Sketch of the rectangular test cell used for the solidification experiment together with measured cooling curves as recorded during the experimental run. The temperatures were measured with six thermocouples inside the narrow sidewalls at different positions (A, B, C, D, E, F), inside the test cell (G), and outside with contact with the plexiglass (H). The corresponding positions are indicated in the sketch by the white/gray dots. The inside dimensions of the test cell were 60 × 40 × 6 cm^3 (h/w/d).

3. Results

Figs. 2-4 show a side view of different parts of the test cell taken at different points in time. The time designations always refer to the start of cooling. Approximately 2600s after the start of cooling, the temperatures measured by the sensors inside the brass sidewalls reach the liquidus temperature of the solution. However, it takes another 1000s before the first crystals become visible on the surface of the narrow sidewalls and in the gasket gap between brass and plexiglass (Fig. 2). Approximately 500 s later, the brass surface is fully covered with crystals. We have suggested terming this stage 'nucleation and growth' [30]. At this stage, no solid forms at the bottom wall, and no equiaxed crystals are visible in the bulk melt.

Fig. 3 shows a sequence of images taken on the right side of the test cell. After the aforementioned 'nucleation and growth' stage, more and more crystals are visible in the two lower-corner regions (left and right). They sink and form two piles of sedimented crystals. For some time, the gradual piling up of crystals at the two bottom corner regions occurs without any visible interaction of the crystals' motion from the opposite cooled sidewall (Fig. 3**b**). It is suggested to term this stage of independent sedimentation in the bottom corner regions as 'corner sedimentation' stage [30]. This stage ends when the crystal motion along both cooled sidewalls starts to interact. During that stage, an increasing number of crystals become visible in the bulk melt. Some of them are traveling upwards to the top of the bath and then downwards again, following vortices that act perpendicular to the plexiglass walls. At approximately 6800 s, these vortices start to sway (not shown) which can be taken as the end of the stage.

With the increasing interaction between the crystals flowing along the left- and right-cooled sidewalls, the motion of the crystals in the bulk

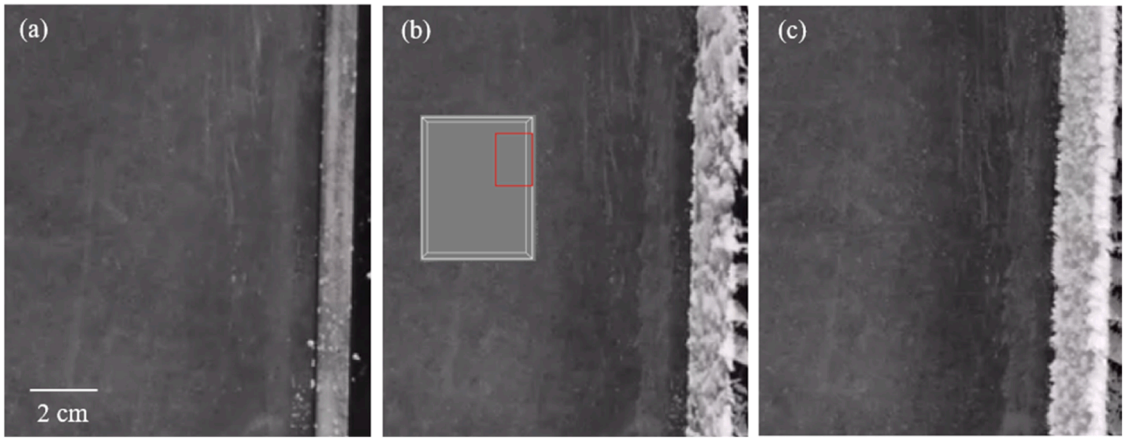

Fig. 2. (a) Nucleation happens at approximately 3600 s on the surface of the narrow sidewalls and in the gasket gap between brass and plexiglass, (b) another 500 s later, the brass surface is completely covered with solid, and (c) another 1000s later, a growing dendritic mushy layer has formed. Many dendrite tips at the forefront of the mushy layer can be seen. The pictures were taken at 3600 s, 4100 s, and 5100 s. The insert indicates the volume of the liquid bath within the test cell and the marked red frame shows the area from where the images were taken.

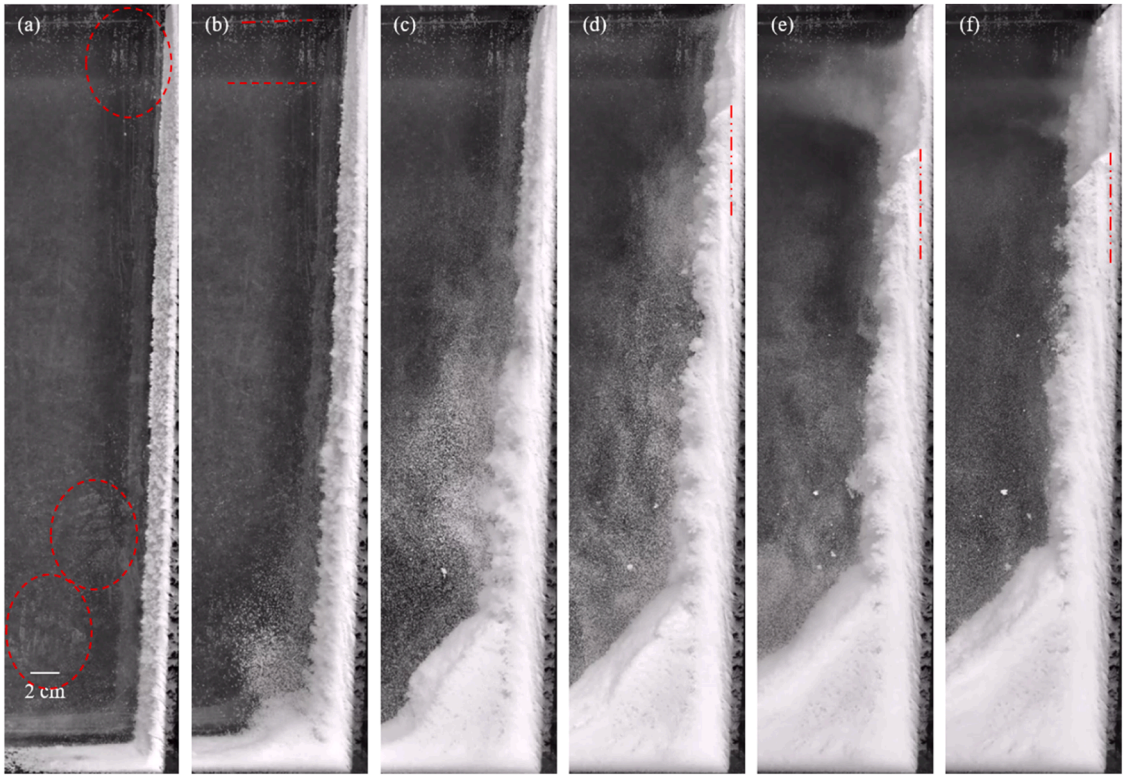

Fig. 3. The sequence of images taken at the right sidewall at (a) 5000 s, (b) 6000 s, (c) 7000 s, (d) 8000 s, (e) 9000 s and (f) 10000s shows the evolution of the vertical mushy layer. The amount and the dynamic of crystals moving in the bulk ahead of the mushy layer increases from (b) to (d) and decreases from (d) to (f) again. An inhomogeneous sedimentation layer at the bottom corner forms that grows with time. The relatively even vertical mushy layer in (a) gets quite fringed in (d-f). In addition, an indentation (bowl-like depression) forms at the upper mushy region in (d). In (e) and (f) this indentation increases in size as its lower part shifts downwards. The flow channel that is related to this indentation is marked by dot-dashed lines in (d-f). Clouds of tiny crystals move horizontally in (e-f) following the flow stratification at the top of the test cell. Bubbles that are adhering to the plexiglass are circled with red dashed ellipses in (a). The surface of the bath is marked with a red dot-dashed line in (b). In addition, an optical reflection that has led to the gray horizontal band is also marked with the red dashed line.

melt becomes irregular and unsteady (Fig. 4). It appears that the flow is 'swinging' from one side to the other, although without perfect rhythmicity. The test cell is now full of equiaxed crystals that occasionally travel upward. Nevertheless, most of the crystals continue to sink, resulting in the perception of 'snowing'. For this reason, this stage is referred to as the 'swinging of turbulent snowing' stage [30]. With time

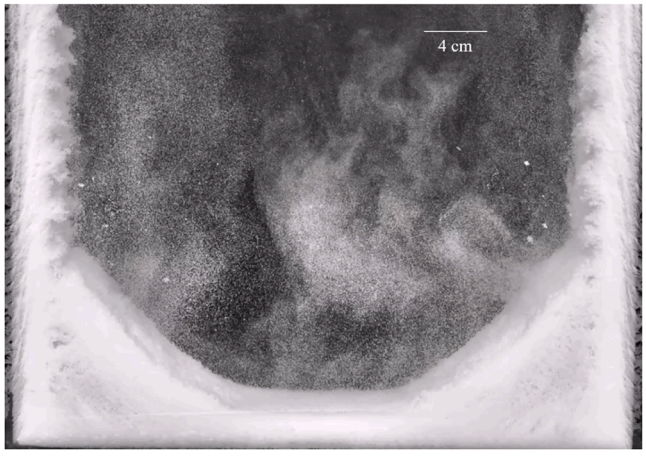

Fig. 4. The lower part of the test cell at approximately 8900 s shows heavily unsteady crystal motion. The sedimentation along both narrow sidewalls is no longer independent of each other. Rather, crystals swirl around far across the middle of the test cell. At a moment a vortex is governed from one side and the next moment from the other side. So the impression occurs that the flow is 'swinging', but without a clear rhythm.

the strength of this unsteady flow stage decreases and the vortices gradually get weaker. The end of that stage is however not so clear to define, especially as an additional phenomenon at the top of the bath gradually becomes more important.

While vortices whirled around the crystals, the flow at the top of the test cell calmed down. A smooth sideward motion develops that transports tiny crystals from left to right and vice versa (meandering-type flow pattern). It starts at around 7500 s by forming the first single horizontal flow layer. With time six to eight layers get visible. This layering indicates the occurrence of a composition and flow stratification. In Fig. 3**d-f** it can be seen that clouds of tiny crystals are following the corresponding flow stratification.

4. Discussion

Several of the described phenomena are well-known, while others are new. It is well established that NH_4Cl crystals that originate from an NH_4Cl-H_2O solution with <80.3 wt.% H_2O, forms equiaxed dendrites with six sidearms that resemble those known from metallic alloys. That is the reason why, for over 50 years, solidification experiments with such solutions have been very common. It is also clear that on solidification, NH_4Cl crystals reject H_2O and that the enrichment of the melt with H_2O lowers its density [5,11–13,17]. Therefore, solutal buoyancy occurs and creates interdendritic flow channels. When cooling happens from the bottom, such flow channels lead to plumes above the solid skeleton [6,12,19,20]. When cooling happens from the side, these flow channels are pointing upwards with some inclination towards the bulk melt [16,17]. For NH_4Cl-H_2O solutions having a composition of around 70 wt.% H_2O (the eutectic is at 80.3 wt.%), solutal buoyancy is much stronger

compared to thermal buoyancy. So, a melt that initially flows downwards along a cooled vertical wall changes direction as soon as solidification has reduced the density of the interdendritic melt. The upward-flowing H_2O-enriched interdendritic liquid leads to the formation of a composition and flow stratification at the top of the cavity [15–17,29].

In the present experiment, upwards-directed flow channels in the vertical mushy layers were observed (at least at the plexiglass walls) along with flow stratification that gradually develops from the surface of the bath downwards as the process progresses (Fig. 3**e-f**). However, the massive occurrence of equiaxed crystals and their interaction with the vertical mushy zone is much more significant in the present experiment compared to what can be found in the literature. The origin of the equiaxed crystals can not be estimated directly. When they become optically visible, their size is already significantly larger than any nucleation radius. Since all visible crystals are in motion, it is reasonable to assume that they did not form at the position where they were first observed. Most of the crystals become visible ahead of the vertical mushy layer while already sedimenting. However, it appears that many crystals were leaving the top part of the vertical mushy zone together with the interdendritic flow that creates the concentration and flow stratification, especially after 7000 s (Fig. 3**d-f**). It is known that interdendritic flow channels are sources of dendritic fragments, transporting both segregated liquid and crystal fragments into the bulk melt [32–36]. In the present experiment, larger crystals that directly sink (Fig. 3**b-c**) can be distinguished from smaller, tiny crystals that move horizontally with the flow. An example of horizontally moving crystals can be seen in the upper part of Fig. 3**e-f** where 'clouds' of crystals are visible. From zooming into the video that refers to Fig. 3**d-e** the impression is created that these 'clouds' of tiny crystals are permanently leaving the upper region of the vertical mush. However, also larger crystals seem to come directly from these areas. They are moving directly downward.

Another interesting observation is that over time, the lower part of the vertical mushy layer becomes increasingly fringed (Fig. 5**a-f**). Generally, dendrite tips define the forefront of a mushy zone. As in the present case more and more equiaxed crystals sink along this boundary, occasionally they get stuck to the dendrite tip front. These now protruding crystals are an obstacle for further crystals that sink along the vertical mushy layer, causing more crystals to become trapped there. This happens until such a crystal agglomeration gets too big and thus collapses. An example of this process can be seen in Fig. 5**f**. The phenomenon described here, first happens around the end of the 'corner sedimentation' stage and continues to occur till the end of the experimental run. It is quite different from the observation of the massive formation of equiaxed crystals by avalanches of mushy zone segments described in our previous work [27] and it is also different from the sliding-down mushy zone segments as described in [30]. The collapsing of crystal agglomerations and the corresponding sudden sliding down contribute to the unsteadiness of the flow in the bulk melt.

Flow channels, that transport segregated interdendritic melt and also crystal fragments, get more and more significant. As the flow channels are inclined towards the bulk melt, they reach the forefront of the vertical mushy layer in the upper part of the test cell. This happens with a significantly higher probability in test cells that are large enough. At

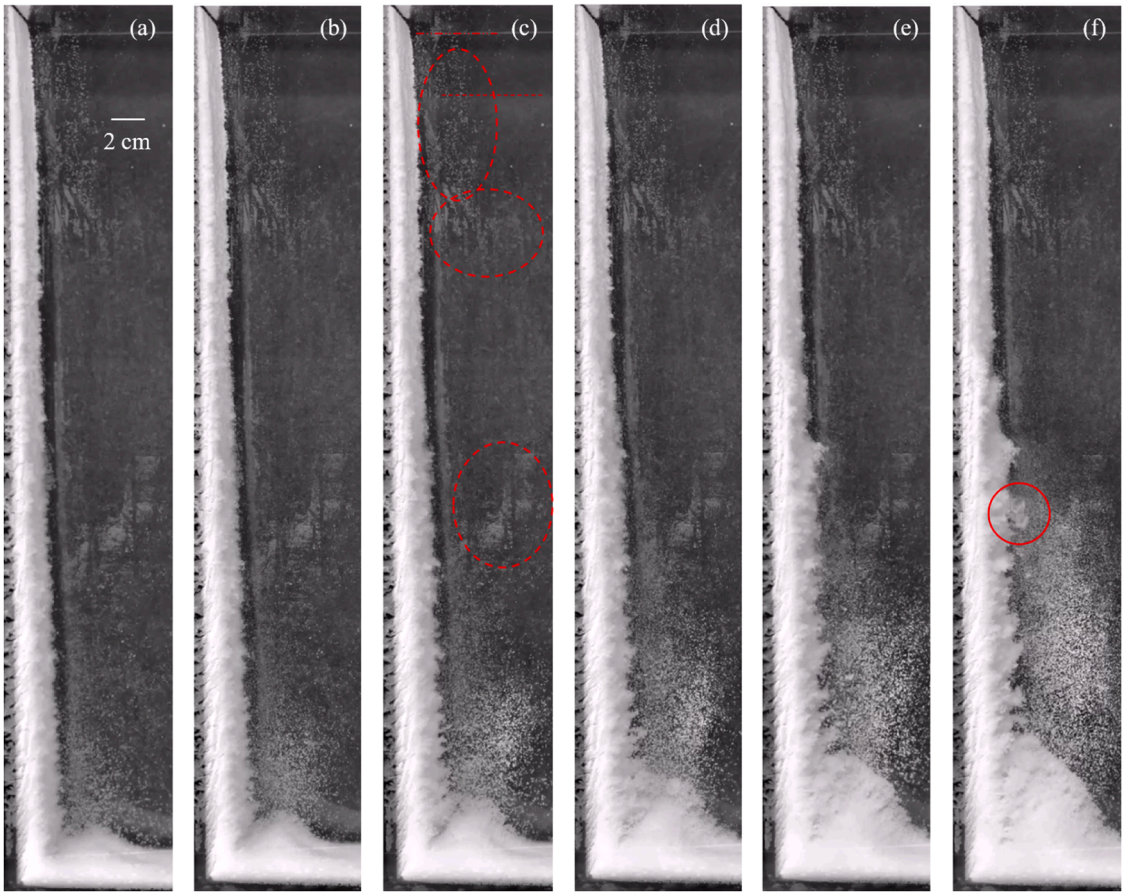

Fig. 5. The sequence of images taken at the region close to the left sidewall at (a) 5900 s, (b) 6000 s, (c) 6100 s, (d) 6200 s, (e) 6300 s and (f) 6400 s shows how the forefront of the vertical mushy layer gets fringed. More and more sinking crystals find a location where they stick to the mushy front. However, the developing crystal agglomerations might get too big and finally become loose again. The agglomeration circled in red in (f) has formed elsewhere and is now already sinking downwards. Bubbles that are adhering to the plexiglass during the entire process are circled with red dashed ellipses in (c). The surface of the bath is also marked with a red dot-dashed line in (c) and an optical reflection that has led to the gray horizontal band is also marked with the red dotted line.

these locations, the segregated interdendritic melt hinders the vertical mushy zone from further solidifying, or it even melts away already existing areas of the mushy skeleton, forming a significant indentation (a bowl-shaped depression). This can be seen in Fig. 3**d-f** and also in Fig. 6, where red dot-dashed lines mark the upper part of two flow channels. Fig. 6 shows another example of how the exit of a flow channel can gradually hinder the vertical mushy zone from further solidifying and even cause remelting. Melting the mushy skeleton around the exit of the flow channel is a process that continues with time. Therefore, the indentation in Fig. 3**d-f** and Fig. 6 went further down. As previously mentioned, segregated liquid and crystal fragments exit the flow channel. The smaller fragments are transported with the liquid whereas the larger fragments directly sediment on the edge of the indentation. From there, depending on the slope of the edge, they either slide down directly or accumulate. In smaller test cells, such indentations occur as well, but they could not be observed as clearly as what occurs in this large test cell [37,38].

Fig. 7 shows two examples that demonstrate the sudden collapse of crystal agglomerations that had formed on the lower edge of an indentation. Similar to the collapse of crystal agglomerations that had formed at the forefront of the vertical mushy layer, the collapse leads to further fragmentation when hitting any position of the front of the mushy region below. Note that during the pileup of such a crystal agglomeration, the flow channel that has formed the indentation might continue to reject highly-segregated liquid and thus favor solutal melting. So, the connection between the agglomeration and the vertical mushy layer might thus not get strong.

With time the meandering-type, double-diffusive flow pattern extends further downwards. At the end of the experimental run almost one-third of the test cell is occupied with a flow stratification as can be seen in Fig. 8. Crystals that swirl around in the lower part of the test cell can not penetrate this flow region. Viewing in this light, the increasing area of double-diffusive convection confines the region where unsteady vortices exist.

Although in recent years progress has been made in numerically modeling complex solidification processes including columnar growth with motion of equiaxed crystals, formation and motion of dendritic fragments, and formation of macrosegregation including flow and concentration stratification, even the most advanced model is unable to describe the processes outlined above. So, the present contribution demonstrates in which directions future numerical models should develop.

The transfer of the present observations to industrial configurations should be done with care. Although, many common alloys like superalloys, steels, and others, reveal solidification-induced solutal buoyancy that leads to a rising interdendritic melt flow and so to A-segregations, freckles, and ghost lines, a relatively large flow-channel-created-indentation in a vertical mushy layer, as reported here, might be rare. Here, the choice of the coldest temperature at 5 °C hindered the dendritic skeleton from further solidifying. Therefore, the higher-segregated interdendritic liquid could relatively easily stop the dendritic skeleton (which has only a solid volume fraction of 15–20 %) from further growth. However, in industrial processes, a reduction in the heat transfer coefficient between casting and mold could also decrease heat transfer and slow down solidification. So, at vertical parts of big castings, the agglomeration of crystals either directly at the vertical front or at other suitable locations might occur and the collapse of such agglomeration might lead to a crystal multiplication and an avalanche-type crystal flow phenomenon similar to the ones described here.

5. Conclusions

The main observations of the described experiment are the following:

- Even in the relatively large test cell, double-diffusive convection occurs that gradually extends from the top of the bath downwards (Fig. 8). This is not self-evident as the large number of equiaxed crystals (fragments) that seem to leave the upper part of the vertical mushy layer constantly could have suppressed concentration and flow stratification.
- Due to the large test cell, interdendritic flow channels leave the vertical mushy layer before reaching the top of the bath. As they transport highly-segregated interdendritic melt, the exit region from the mushy layer is vigorously affected. The channels hinder the mushy zone from further solidifying or even cause remelting of already existing areas and so form quite large indentations into the mushy layer.
- Two mechanisms are discussed that lead to the sliding down of larger crystal agglomerations. First, crystals that sink along the vertical mushy layer may stuck to protruding dendrites. Crystals that follow are also stopped and fixed until an agglomeration forms that gets too large. Second, the lower edge of the flow-channel-induced indentation can serve as a location where sinking crystals sediment. Again, after reaching a certain size, the agglomeration collapses. The sinking crystal agglomeration further interacts with the lower mushy

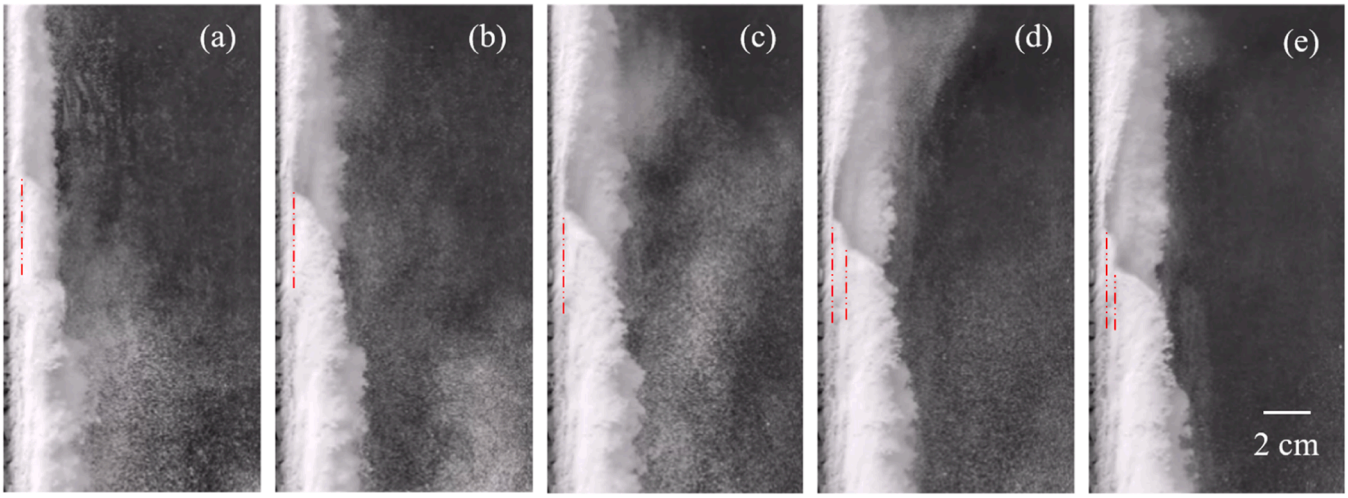

Fig. 6. The sequence of images taken at the upper left sidewall at (a) 7000 s, (b) 7800 s, (c) 8600 s, (d) 9400 s, and (e) 10200s shows the formation and widening of an indentation at the mushy layer. The process is caused by the rising interdendritic melt that is leaving the mushy region via one flow channel, and later even two flow channels. Their upper parts are marked with dot-dashed red lines. Generally, flow channels appear gray in these pictures.

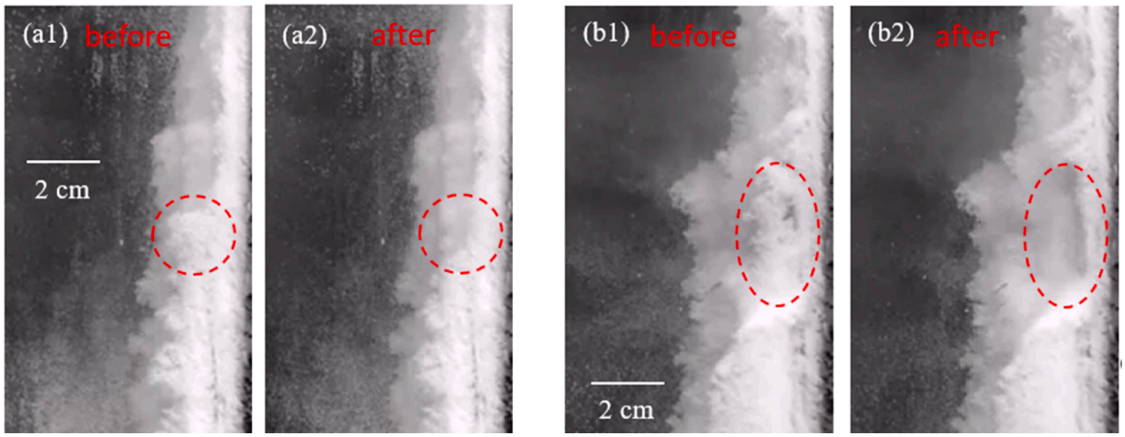

Fig. 7. The two pairs of pictures (a1-a2) and (b1-b2) show the collapse of crystal agglomerations that had pileup on the lower edge of an indentation. The dashed red circles/ellipses mark the areas before and after the agglomerations collapse. The pictures were taken at 8056 s and 8080 s (a1-a2), and 12064s and 12114s (b1-b2).

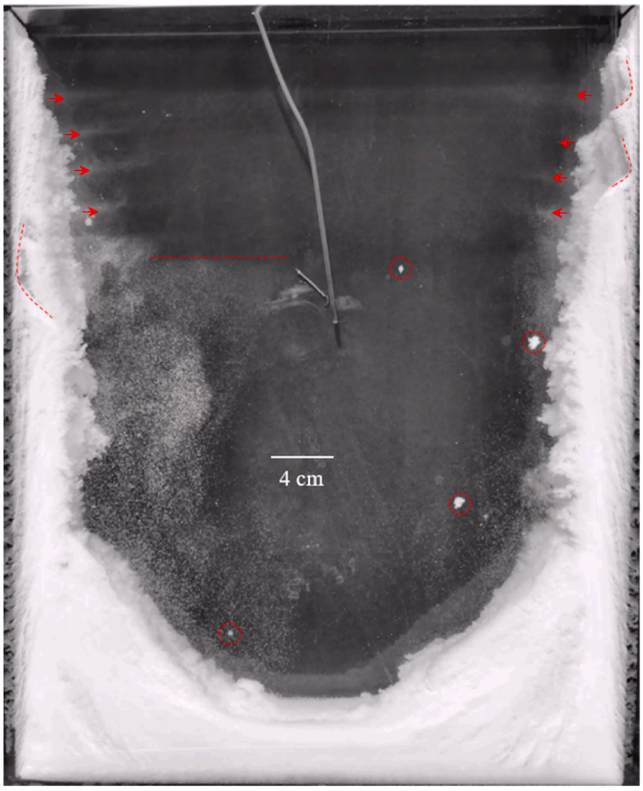

Fig. 8. The picture shows the test cell at 14200s. The red arrows mark the flow direction of the concentration and flow stratification visible by the motion of 'clouds' of tiny crystals. Indentations created by interdendritic flow channels are marked with red dashed curves. On the right side, the two indentations are still 'empty', while on the left side, the indentation is filled with a crystal agglomeration. The horizontal dashed line marks the lower limit of the flow stratification, which is also an upper limit for rising larger crystals from below. Crystals that in the meantime adhere to the plexiglass are marked with red dashed circles.

layer and heavy fragmentation is the consequence. This is the reason why the occurrence of equiaxed crystals is quite unsteady. Especially the avalanche-type sudden downward motion of a large amount of crystals leads to an unsteady sedimentation layering as can be seen in the lower part of Fig. 8.

The observations show that in technical processes, but also in processes that occur in nature, the occurrence of uneven structures might be caused by a complex interplay of different phenomena. Here, flow and concentration stratification, segregation channels, collapsing of crystal agglomerations/mushy zone segments, and unsteady flow vortices lead to a sedimentation bed that is far from being homogenous.

CRediT authorship contribution statement

Andreas Ludwig: Writing – review & editing, Validation, Supervision, Project administration, Conceptualization. **Golshan Shayesteh:** Investigation, Writing – original draft. **Mihaela Stefan-Kharicha:** Validation, Investigation. **Menghuai Wu:** Writing – review & editing. **Abdellah Kharicha:** Writing – review & editing.

Declaration of competing interest

The authors declare that they have no known competing financial interests or personal relationships that could have appeared to influence the work reported in this paper.

Acknowledgments

The authors express their gratitude to Montanuniversitaet Leoben for sponsoring this work within the framework of a recent doctoral program.

On behalf of all authors, the corresponding author states that there is no conflict of interest.

Supplementary materials

Supplementary material associated with this article can be found, in the online version, at doi:10.1016/j.ijheatmasstransfer.2024.126638.

Data availability

No data was used for the research described in the article.

References

[1] S.C. Huang, M.E. Glicksman, Overview 12: fundamentals of dendritic solidification-I. Steady-state tip growth, Acta Metall. 29 (1981) 701–715, https://doi.org/10.1016/0001-6160(81)90115-2.
[2] K.A. Jackson, J.D. Hunt, Lamellar and rod eutectic growth, Trans. AIME 236 (1966) 1129–1141.
[3] K.A. Jackson, J.D. Hunt, Binary eutectic solidification, Trans. AIME 237 (1966) 843–852.

[4] S. Akamatsu, H. Nguyen-Thi, In situ observation of solidification patterns in diffusive conditions, Acta Mater. 108 (2016) 325–346, https://doi.org/10.1016/j.actamat.2016.01.024.
[5] S.M. Copley, A.F. Giamei, S.M. Johnson, M.F. Hornbecker, M. Copley, The origin of freckles in unidirectionally solidified castings, Met. Trans. 1 (1970) 2193–2204.
[6] R.J. McDonald, J.D. Hunt, Convective fluid motion within the interdendritic liquid of a casting, Met Trans. 1 (1970) 1787–1788, https://doi.org/10.1007/bf02642039.
[7] J. Szekely, A.S. Jassal, An experimental and analytical study of the solidification of a binary dendritic system, Metall. Trans. B. 9 (1978) 389–398, https://doi.org/10.1007/BF02654412.
[8] T. Motegi, A. Ohno, Origin of showering crystals in the molten metal in a mold cooled from the top, J. Japan Inst. Met. Mater. 44 (1980) 359–366, https://doi.org/10.2320/jinstmet1952.44.4_359.
[9] A. Ohno, T. Motegi, T. Shimizu, The formation of equiaxed crystals in ammonium chloride-water model and Al alloy ingots by electromagnetic stirring, J. Japan Inst. Met. Mater. 46 (1982) 554–563, https://doi.org/10.2320/jinstmet1952.46.5_554.
[10] A. Ohno, Solidification - The Separation Theory and Its Practical Applications, Springer Berlin Heidelberg, 1984, https://doi.org/10.1007/978-3-642-95537-2.
[11] A. Sample, A. Hellawell, The effect of mold precession on channel and macro-segregation in ammonium chloride-water analog castings, Metall. Trans. B. 13 (1982) 495–501, https://doi.org/10.1007/BF02667766.
[12] A. Sample, A. Hellawell, Mechanisms of formation and prevention of channel segregation during alloy solidification, Metall. Trans. A, Phys. Metall. Mater. Sci. 15 A (1984) 2163–2173, https://doi.org/10.1007/bf02647099.
[13] C. Beckermann, R. Viskanta, Double-diffusive convection due to melting, Int. J. Heat Mass Transf. 31 (1988) 2077–2089, https://doi.org/10.1016/0017-9310(88)90118-4.
[14] C. Beckermann, R. Viskanta, An experimental study of melting of binary mixtures with double-diffusive convection in the liquid, Exp. Therm. Fluid Sci. 2 (1989) 17–26, https://doi.org/10.1016/0894-1777(89)90045-9.
[15] C. Beckermann, R. Viskanta, An experimental study of solidification of binary mixtures with double-diffusive convection in the liquid, Chem. Eng. Commun. 85 (1989) 135–156, https://doi.org/10.1080/00986448908940352.
[16] M.S. Christenson, W.D. Bennon, F.P. Incropera, Solidification of an aqueous ammonium chloride solution in a rectangular cavity- II. Comparison of predicted and measured results, Int. J. Heat Mass Transf. 32 (1989) 69–79, https://doi.org/10.1016/0017-9310(89)90091-4.
[17] M.S. Christenson, F.P. Incropera, Solidification of an aqueous ammonium solution in a rectangular cavity- l. Experimental study, Int. J. Heat Mass Transf. 32 (1989) 47–68, https://doi.org/10.1016/0017-9310(89)90090-2.
[18] C.F. Chen, F. Chen, Experimental study of directional solidification of aqueous ammonium chloride solution, J. Fluid Mech. 227 (1991) 567–586, https://doi.org/10.1017/S0022112091000253.
[19] A. Hellawell, J.R. Sarazin, R.S. Steube, Channel convection in partly solidified systems, Philos. Trans. A. 345 (1993) 507–544, https://doi.org/10.1098/rsta.1993.0143.
[20] C.S. Magirl, F.P. Incropera, Flow and morphological conditions associated with unidirectional solidification of aqueous ammonium chloride, J. Heat Transf. 115 (1993) 1036–1043, https://doi.org/10.1115/1.2911358.
[21] M.G. Worster, Convection in mushy layers, Ann. Rev. Fluid Mech. 29 (1997) 91–122, https://doi.org/10.1146/annurev.fluid.29.1.91.
[22] J.W. Gao, C.Y. Wang, An experimental investigation into the effects of grain transport on columnar to equiaxed transition during dendritic alloy solidification, J. Heat Transf. 121 (1999) 430–437, https://doi.org/10.1115/1.2825996.
[23] H. Zhong, Y. Zhang, X. Chen, C. Wu, Z. Wei, Q. Zhai, In situ observation of crystal rain and its effect on columnar to equiaxed transition, Metals 6 (2016), https://doi.org/10.3390/met6110271, 271/1–9.
[24] J. Hutt, D. St John, The origins of the equiaxed zone -Review of theoretical and experimental work, Int. J. Cast Met. Res. 11 (1998) 13–22, https://doi.org/10.1080/13640461.1998.11819254.
[25] I. Thakur, S. Karagadde, A. Srivastava, Mechanisms leading to the formation of double-diffusive layers during unidirectional solidification of aqueous NH4Cl solution, Phys. Rev. Fluids 7 (2022), https://doi.org/10.1103/PhysRevFluids.7.063501, 063501/1–27.
[26] I. Thakur, S. Karagadde, A. Srivastava, In-situ characterization of double-diffusive convection during unidirectional solidification of a binary solution, Exp. Heat Transf. 37 (2024) 495–522, https://doi.org/10.1080/08916152.2022.2163434.
[27] A. Ludwig, M. Stefan-Kharicha, A. Kharicha, M. Wu, Massive formation of equiaxed crystals by avalanches of mushy zone segments, Met. Mater. Trans. A. 48 (2017) 2927–2931, https://doi.org/10.1007/s11661-017-4008-y.
[28] A. Kharicha, M. Stefan-Kharicha, A. Ludwig, M. Wu, Simultaneous observation of melt flow and motion of equiaxed crystals during solidification using a dual phase particle image velocimetry technique. Part II: relative velocities, Met. Mater. Trans. A. 44 (2013) 661–668, https://doi.org/10.1007/s11661-012-1415-y.
[29] A. Kharicha, M. Stefan-Kharicha, A. Ludwig, M. Wu, Simultaneous observation of melt flow and motion of equiaxed crystals during solidification using a dual phase particle image velocimetry technique. part I: stage characterization of melt flow and equiaxed crystal motion, Met. Mater. Trans. A. 44 (2013) 650–660.
[30] G. Shayesteh, A. Ludwig, M. Stefan-Kharicha, M. Wu, A. Kharicha, On the conditions for the occurrence of crystal avalanches during alloy solidification, J. Phys. Conf. Ser. 2766 (2024), https://doi.org/10.1088/1742-6596/2766/1/012199, 012199/1–6.
[31] M. Stefan-Kharicha, A. Kharicha, J. Mogeritsch, M. Wu, A. Ludwig, Review of ammonium chloride-water solution properties, J. Chem. Eng. Data. 63 (2018) 3170–3183, https://doi.org/10.1021/acs.jced.7b01062.
[32] H. Jung, N. Mangelinck-Noël, H. Nguyen-Thi, N. Bergeon, B. Billia, A. Buffet, G. Reinhart, T. Schenk, J. Baruchel, Fragmentation in an Al–7 wt-%Si alloy studied in real time by X-ray synchrotron techniques, Int. J. Cast Met. Res. 22 (2009) 208–211, https://doi.org/10.1179/136404609X367731.
[33] N. Shevchenko, S. Boden, G. Gerbeth, S. Eckert, Chimney formation in solidifying Ga-25wt pct in alloys under the influence of thermosolutal melt convection, Met. Mater. Trans. A. 44 (2013) 3797–3808, https://doi.org/10.1007/s11661-013-1711-1.
[34] S. Karagadde, L. Yuan, N. Shevchenko, S. Eckert, P.D. Lee, 3-D microstructural model of freckle formation validated using in situ experiments, Acta Mater. 79 (2014) 168–180, https://doi.org/10.1016/j.actamat.2014.07.002.
[35] G. Reinhart, H. Nguyen-Thi, N. Mangelinck-Noël, J. Baruchel, B. Billia, In situ investigation of dendrite deformation during upward solidification of Al-7wt.%Si, JOM 66 (2014) 1408–1414, https://doi.org/10.1007/s11837-014-1030-z.
[36] N. Shevchenko, O. Roshchupkina, O. Sokolova, S. Eckert, The effect of natural and forced melt convection on dendritic solidification in Ga-In alloys, J. Cryst. Growth. 417 (2015) 1–8, https://doi.org/10.1016/j.jcrysgro.2014.11.043.
[37] M. Wu, M. Stefan-Kharicha, A. Kharicha, A. Ludwig, Numerical investigation of an in-situ observed flow regime during solidification of an NH4Cl - 70 wt%H2O solution, IOP Conf. Ser. Mater. Sci. Eng. 861 (2020), https://doi.org/10.1088/1757-899X/861/1/012041.
[38] M. Wu, M. Stefan-Kharicha, A. Kharicha, A. Ludwig, Flow-solidification interaction: a numerical study on solidification of NH4Cl–70 wt.%H2O solution in a water-cooled mould with a large sample thickness, Int. J. Heat Mass Transf. 164 (2021) 120566, https://doi.org/10.1016/j.ijheatmasstransfer.2020.120566.